

Synergistic Multiscale Detail Refinement via Intrinsic Supervision for Underwater Image Enhancement

Dehuan Zhang^{1*}, Jingchun Zhou^{1*}, Weishi Zhang¹ [†], ChunLe Guo², Chongyi Li^{2*}

¹ Dalian Maritime University, China

² TMCC, CS, Nankai University, China

zhangdehuan@dlmu.edu.cn, zhouchingchun03@gmail.com, teesiv@dlmu.edu.cn, guochunle@nankai.edu.cn, lichongyi25@gmail.com

Abstract

Visual restoration of underwater scenes is crucial for visual tasks, and avoiding interference from underwater media has become a prominent concern. In this work, we present a synergistic multiscale detail refinement via intrinsic supervision (SMDR-IS) to recover underwater scene details. The low-degradation stage provides multiscale detail for original stage, which achieves synergistic multiscale detail refinement through feature propagation via the adaptive selective intrinsic supervised feature module (ASIF). ASIF is developed using intrinsic supervision to precisely control and guide feature transmission in the multi-degradation stages. ASIF improves the multiscale detail refinement while reducing interference from irrelevant scene information from the low-degradation stage. Additionally, within the multi-degradation encoder-decoder of SMDR-IS, we introduce a bi-focal intrinsic-context attention module (BICA). This module is designed to effectively leverage multi-scale scene information found in images, using intrinsic supervision principles as its foundation. BICA facilitates the guidance of higher-resolution spaces by leveraging lower-resolution spaces, considering the significant dependency of underwater image restoration on spatial contextual relationships. During the training process, the network gains advantages from the integration of a multi-degradation loss function. This function serves as a constraint, enabling the network to effectively exploit information across various scales. When compared with state-of-the-art methods, SMDR-IS demonstrates its outstanding performance. Code will be made publicly available.

Introduction

Amidst the intricate and dynamic underwater environments, the considerable influence of dissolved and suspended matter on light absorption and scattering remains the primary determinant of underwater optical image quality (Guo et al. 2023). Among these factors, absorption effects contribute to challenges such as shortened imaging distances and color distortion, while scattering effects contribute to reduced image contrast and the loss of fine details. We aim to improve underwater optical image quality, offering robust image processing solutions for applications including underwater re-

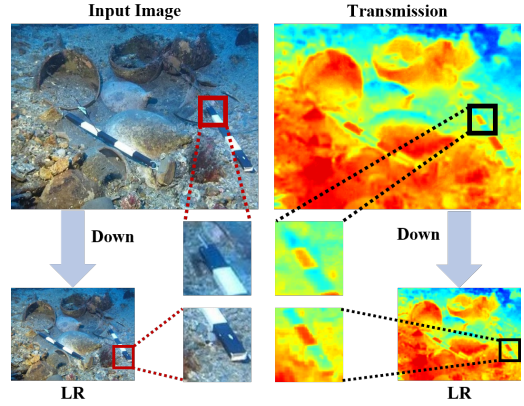


Figure 1: Motivation. Similar scene information from multi-resolution images and transmission. Likewise, comparable degradation patterns occurring at different positions are observable in both the original resolution and low-resolution images.

source exploration, marine biology research, and underwater surveillance (Liu et al. 2022b). Image enhancement methods aid scientific researchers and practitioners in gaining a deeper comprehension and analysis of image data within underwater environments (Kang et al. 2022).

Underwater image enhancement is a challenging task within the field of computer vision, particularly due to the presence of scattering and blurring effects in water environments, which exhibit a multi-scale nature. Suspended particles and turbulence at various scales contribute to diverse degrees of influence on different portions of the image, resulting in degraded multi-scale correlated features. The underwater image formation model (UIM) is as follows:

$$I = J \times t + A(1-t) \quad (1)$$

where I represents a clear image, J denotes an underwater image, t is the transmission, which is related to depth. A represents the atmosphere.

The aim of underwater image enhancement is to estimate the I from Eq. (1) (Zhou et al. 2023a), as the degradation phenomena across different pixel positions in underwater

*These authors contributed equally.

[†]Corresponding author

images vary due to distance-related. Many underwater image enhancement methods (Zhuang, Li, and Wu 2021) employ global or local feature extraction (Liu et al. 2022a) (Liu et al. 2023), utilizing filters (Zhou et al. 2023b) and color correction techniques (Zhou et al. 2022) to improve image quality. However, as seen in Figure 1, considering the inherent scale-relatedness within underwater image scenes (Jiang et al. 2020)(Hou et al. 2023), where different pixel positions exhibit the same level of degradation under consistent depth information, a better understanding of the scene structure can be attained bases on the multi-degradation scene. Consequently, we propose synergistic multiscale detail refinement via intrinsic supervision for underwater image enhancement (SMDR-IS). SMDR-IS introduces the low-resolution images as auxiliary inputs to provide supplementary scene degradation information.

SMDR-IS employs multi-degradation simultaneously, which aids in alleviating the loss of detail features arising from multiple feature extractions. Meanwhile, the low-degradation stages prevent excessive abstraction caused by redundant feature extraction, preserving the inherent relationship between features and the original image. After the feature extraction in the original resolution stage, high-level features are obtained. While these high-level features from the original resolution encoder may capture general data characteristics, they could also lose task-specific crucial information. Introducing the low-degradation image and the features extracted at shallow layers can enhance credibility and applicability. Additionally, the use of ASISF ensures that irrelevant information is not introduced into the original resolution.

The contributions are summarized as follows:

(1) Instead of the insufficient utilization of scale-related features in existing underwater image enhancement methods, which leads to inaccurate restoration of scene details, we propose the framework of synergistic multiscale detail refinement via intrinsic supervision for underwater image enhancement.

(2) The bifocal intrinsic-context attention is designed using a dual-path strategy, effectively catering to both feature enhancement and contextual semantic information. Moreover, resolution-guided supervision is seamlessly integrated, enhancing the model's computational efficiency without compromising the quality of detail enhancement.

(3) To further refine the effectiveness of low-resolution feature information, the adaptive selective intrinsic supervised feature module (ASISF) is designed to regulate feature propagation. ASISF aims to improve the efficacy of image enhancement and prevent information blurring caused by the superposition of multiscale scene information.

(4) By incorporating a multi-degradation loss function to constrain the network, we facilitate feature optimization and constraints at each stage. This enables the network to better leverage information across diverse scales, thereby enhancing the ability to recover details and structures.

Related Work

Underwater image enhancement methods have been widely applied in computer vision and image processing (Zhuang

et al. 2022). Underwater image enhancement methods based on deep learning can be categorized into methods based on prior and end-to-end methods.

Enhancement Based on Prior

Methods based on priors necessitate explicit degradation models or prior knowledge to train model parameters. For instance, in (Li et al. 2021), UColor is proposed based on transmission, which employs a transmission-guided image enhancement network using the GDCP-based transmission (Peng, Cao, and Cosman 2018). (Zhou et al. 2023c) takes inputs such as the original image, color-corrected image, and contrast-enhanced image, the inputs are fused using an improved U-Net to leverage features. USUIR (Fu et al. 2022a) involves designing a transmission subnet, global background subnet, and scene radiance subnet to estimate parameters from UIFM, facilitating real image restoration. Zhang et al. proposed Rex-Net (Zhang et al. 2023), which employs the Retinex theory to assist in enhancing underwater scene images. Although these methods have achieved success, the complexity and uncertainties of underwater environments might render priors ineffective, thereby limiting the model's generalization capabilities.

End-to-end Enhancement

End-to-end underwater image enhancement methods do not require explicit degradation models or prior knowledge. UIEC2 (Wang et al. 2021) enhanced image in the RGB and HSV color spaces. RGB pixel-level blocks are used for color restoration, while saturation is adjusted using curves in HSV. In (Zhou, Zhang, and Zhang 2023), an enhancement method is devised based on cross-view images, which employs feature alignment to fuse scene information from multiple perspectives. Furthermore, a new underwater image dataset is introduced. (Fu et al. 2022b) proposed a consensus-based approach for underwater image restoration, which solved mitigating biases introduced through reference image annotations. (Jiang et al. 2022b) proposed an image-aware adversarial fusion network based on object detection, which incorporated a multi-scale dense enhancement subnet to enhance visual results, (Jiang et al. 2022b) introduced global-local adversarial during image reconstruction to leverage image context information effectively. However, existing end-to-end underwater image enhancement methods ignore adequately utilizing scale-related features of image scenes, leading to challenges in accurately recovering scene details. Therefore, we propose SMDR-IS based on the synergistic multiscale detail and intrinsic supervision.

Methodology

We proposed Synergistic Multiscale Detail Refinement via Intrinsic Supervision for Underwater Image Enhancement (SMDR-IS), as illustrated in Figure 2. SMDR-IS contains the multi-degradation encoder and multi-degradation decoder.

Multi-Degradation Encoder

We design four stages of multi-resolution image inputs to provide the network with various scale scene information

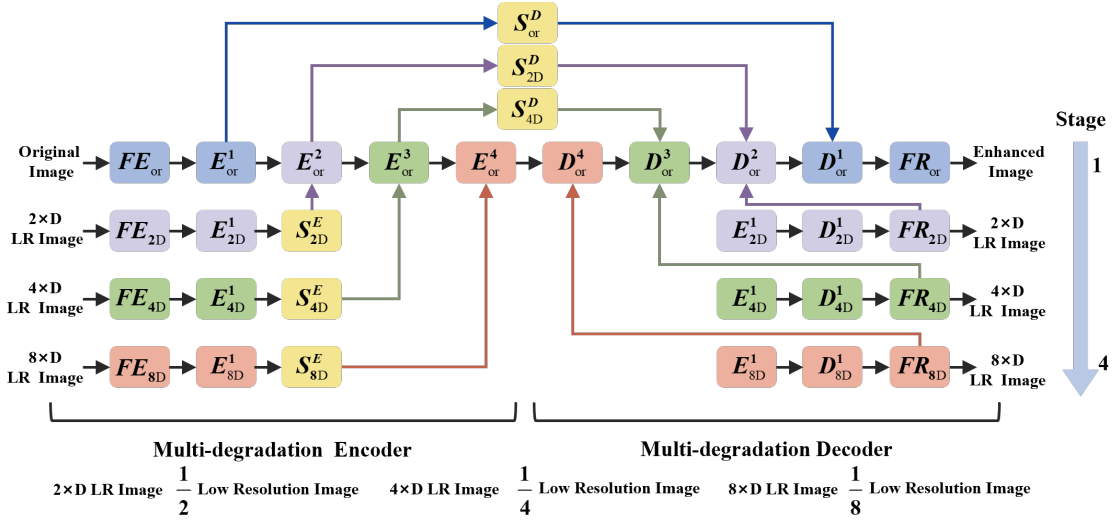


Figure 2: The overview of SMDR-IS. FE_i is Feature Extract (Conv). E_i^1, D_j^1 denotes the Bifocal Intrinsic-Context Attention (BICA). $E_i^i, i \in [2, 4]$ is Downsampling+BICA. $D_j^i, i \in [2, 4]$ is Upsampling+BICA. S Adaptive Selective Intrinsic Supervised Feature Module (ASISF). FR_{or} is Feature Restoration(Conv). $FR_j, j \in \{2D, 4D, 8D\}$ denotes Conv+ASISF.

and scale-relatedness feature. Firstly, we use downsampling in the original image to obtain different scale underwater scene inputs. Based on the existing UNet-based underwater image enhancement methods (Li et al. 2021) that commonly use three downsampling steps, we employ four stages to capture different scale scene information, which contains the original image and three downsampling low-resolution images. To exploit the scale-correlated features of the image scene, SMDR-IS introduces the original resolution encoder and utilizes three low-resolution image stages to provide different scale underwater scene information.

In each encoder, we design the bifocal intrinsic-context attention module (BICA) to enhance the details of the features. BICA efficiently integrates global and local features for underwater image enhancement. By leveraging resolution-guided supervision, BICA achieves an optimal balance between computational efficiency and superior detail quality.

To further constrain the effectiveness of low-resolution feature information, we propose the adaptive selective intrinsic supervised feature module (ASISF) to control feature propagation. ASISF can improve the performance of image enhancement, and prevent information blurring caused by overlaying multi-scale scene information.

Bifocal Intrinsic-Context Attention The bifocal intrinsic-context attention module (BICA) comprises two branches, the architecture of BICA is shown in Figure 3. In Branch 1, acknowledging the pronounced reliance of image restoration on neighboring pixel regions, we incorporate the comprehensive feature attention (CFA) module (seen in supplementary material) to initially extract pixel and channel features. Subsequently, the resolution-guided intrinsic attention module (ReGIA) is designed to expand receptive fields while ensuring time efficiency. ReGIA employs low-resolution spatial intrinsic supervision to enrich the high-resolution space, acquiring multi-scale scene detail information.

In Branch 2, recognizing the substantial dependence of underwater image restoration on spatial contextual relationships, we design the hierarchical context-aware feature extraction module (seen in supplementary material). This module operates within the original feature space, extracting image representation features using distinct receptive fields.

BCIA integrates channel and spatial attention through the innovative dual-path attention mechanism, enhancing the extraction and fusion of both global and local image features. By employing a resolution-guided supervision strategy, BCIA elevates computational efficiency without compromising the quality of details. The singular fusion of global context and local nuances within BCIA, combined with its seamless integration into existing models, establishes BCIA as a seminal development in the field of underwater image enhancement.

Resolution-Guided Intrinsic Attention Module Optimizing underwater imagery heavily relies on the contextual information of neighboring pixels. However, to manage network complexity, enhancement approaches often utilize the compact 3×3 convolutional kernel during the feature extraction process. While the 3×3 convolutional kernel is efficient, it inherently restricts the network’s receptive field, thereby limiting its capacity to capture broader contextual information.

To overcome the limitation and broaden the network’s receptive field, we propose the resolution-guided intrinsic attention module (ReGIA) after the initial feature extraction from the original space. The ReGIA is designed to extract feature weight in the lower-resolution and large receptive field latent space. By expanding the convolutional kernel’s receptive field, ReGIA serves as a guidance mechanism that enhances the feature correlation within the original feature space, leveraging its reference in the expanded context.

Adaptive Selective Intrinsic Supervised Feature Module

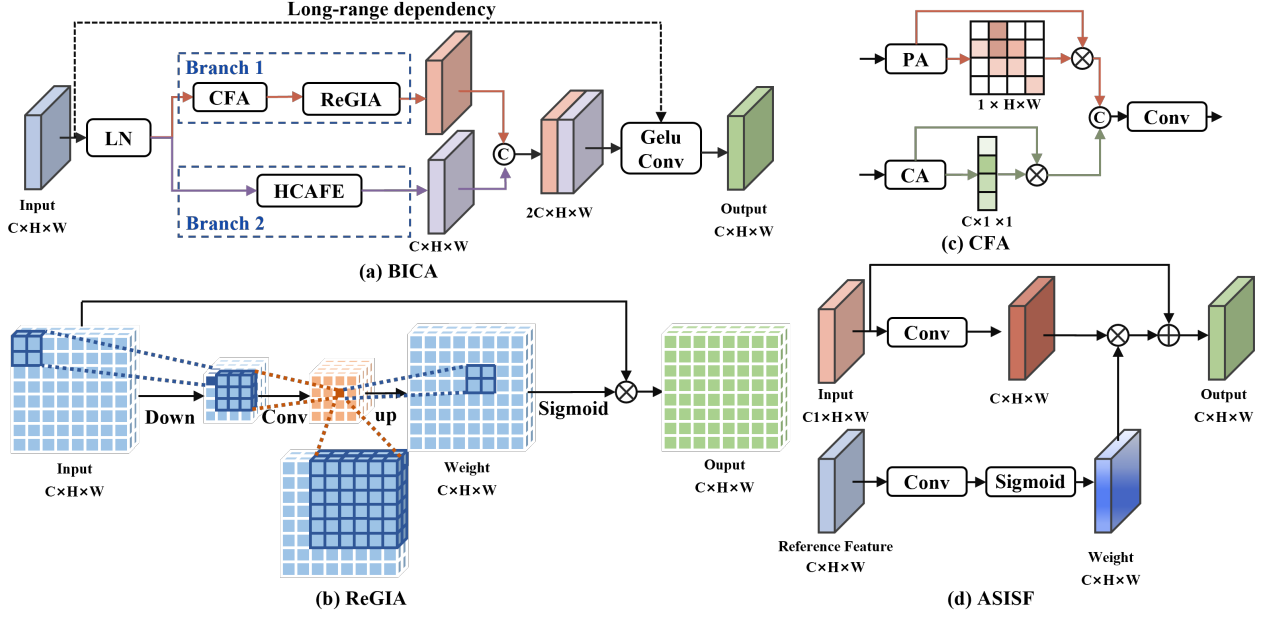


Figure 3: (a) The architecture of BICA, LN is Layer Normalization. (b) ReGIA, down and up are downsampling and upsampling, respectively. In low-resolution, 1×1 can refer to the 6×6 spatial feature in the original resolution. (c) CFA, CA is Channel Attention, and PA denotes Pixel Attention. (d) ASISF. The channels in the input and reference features can vary.

In the process of integrating feature information from the low-resolution encoder and decoder into the original resolution branch, it is essential to prevent interference from irrelevant data during the image restoration phase (Zamir et al. 2021). Therefore, we design an adaptive selective intrinsic supervised feature module (ASISF), which employs the intrinsic-supervised approach to feature selection and constraint, as seen in Figure 3.

ASISF applies a meticulous strategy to ensure that only the most relevant features are preserved for the processing in original resolution stage. While extracting features from the low-resolution encoder, the features from the original resolution serve as reference features. In the encoder, we employ the output of SMDR-IS as the reference feature, which is utilized to constrain the process of the low-resolution encoder-decoder. Furthermore, the utilization of multi-degradation ground truth and the comparison between the SMDR-IS's output and multi-degradation images are leveraged to enforce intrinsic supervision. This approach ensures that the multi-degradation encoder and decoder components remain constrained and aligned with the actual degradation characteristics present in the underwater images. This alignment is crucial for the network to learn and generalize effectively, leading to improved performance in restoring the image.

This is particularly significant in the context of image restoration, where the presence of noise, distortions, and varying degradation levels can complicate the recovery process. By employing intrinsic-supervised, ASISF effectively identifies and retains features that contribute meaningfully to the restoration task, thereby ASISF enhances the precision and efficiency of the restoration process.

Multi-Degradation Decoder

SMDR-IS designs the multi-degradation decoder to complement the multi-degradation encoders, which introduces a unique approach distinct from traditional UNet architectures. Low-degradation information encapsulates the degraded aspects of the input image, which are typically caused by various factors such as noise, blurriness, or compression artifacts. Incorporating this information into the decoder allows the network to better understand and address these specific degradation patterns.

By fusing low-degradation information alongside the residual information provided by the encoder, the multi-degradation decoder gains a more comprehensive understanding of the image's degradation characteristics. Multi-degradation encoder enables the network to generate restoration results that are more accurate and contextually meaningful. Essentially, the low-degradation information serves as an additional cue that guides the decoder in enhancing the restoration process. As a result, the generated images not only retain fine details but also effectively restore various forms of degradation. Certainly, it's also noteworthy that within the FR_{iD} framework, the ASISF is utilized to perform intrinsic-supervised feature selection on the output features when providing information to the original degradation encoder. ASISF assists ensure relevant feature information is propagated throughout the image processing pipeline.

In summary, the network's capacity to address and rectify diverse degradation factors is enhanced by leveraging low-degradation information in the decoder of SMDR-IS, which ultimately leads to an overall improvement in the quality of the restored images.

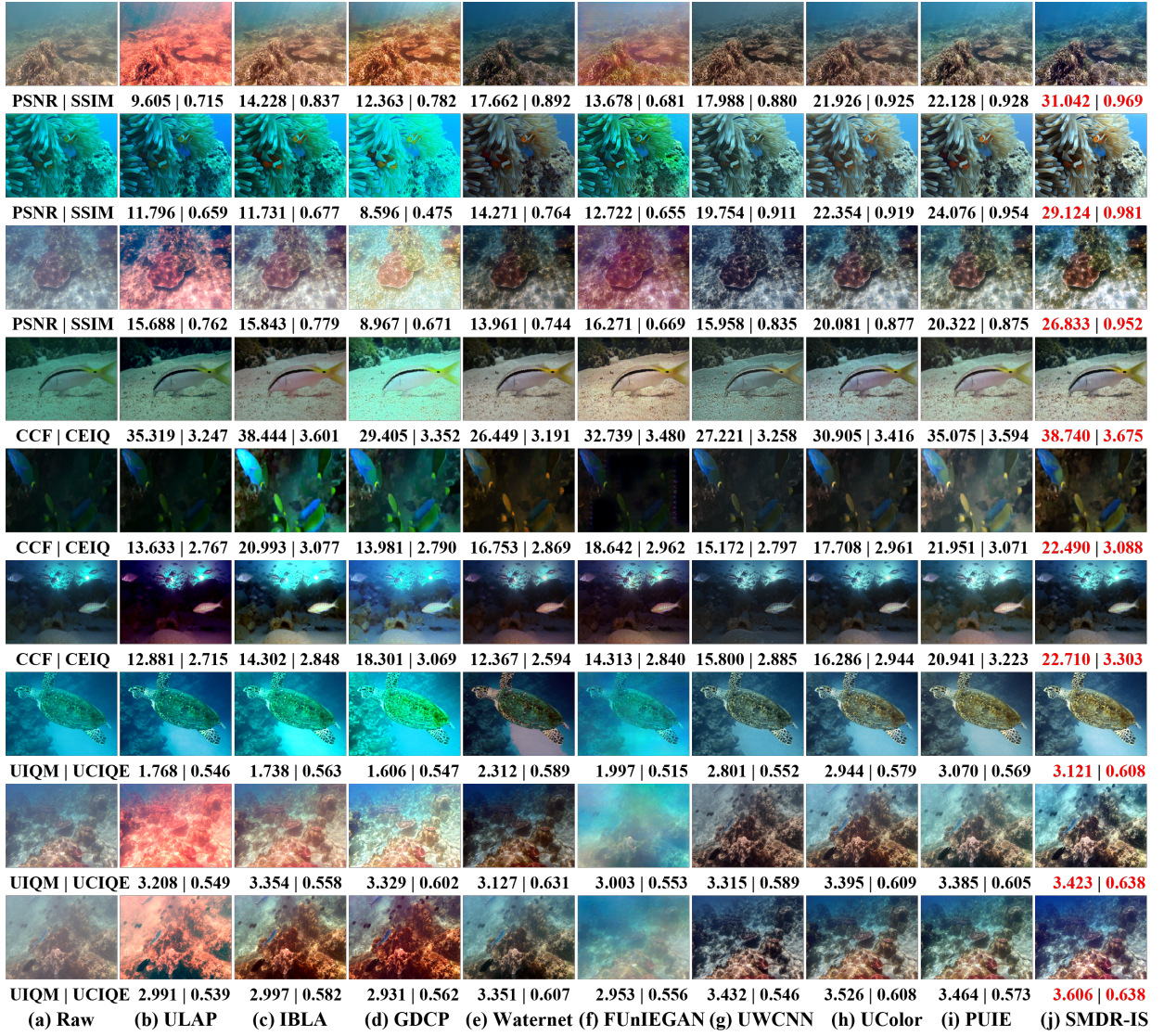


Figure 4: Subjective comparisons between state-of-the-art methods and the proposed SMDR-IS on the different testing datasets. From top to down: 1-3 are from UIEB Val, 4-6 are from UIEB Test, and 7-9 are from U45.

Multi-Degradation Loss Function

To ensure the accuracy of the restoration process, SMDR-IS employs a multi-degradation loss function to regulate the stages. SMDR-IS employs a combination of the L_1 loss function, perceptual loss L_{pre} , and MSE loss L_{mse} , achieving a harmonious optimization process.

$$L_1 = \sum_{i=1}^N |y_i - \hat{y}_i| \quad (2)$$

$$L_{pre} = \sum_{i=1}^M \frac{1}{W_i H_i} \|\phi(y)_i - \phi(\hat{y})_i\|_2^2 \quad (3)$$

$$L_{mse} = \frac{1}{N} \sum_{i=1}^N (y_i - \hat{y}_i)^2 \quad (4)$$

$$L_i = L_1^i + 0.2 \times L_{pre}^i + L_{mse}^i \quad (5)$$

where N is the total number of pixels in the image, y_i denotes the ground truth pixel value, \hat{y}_i represents the predicted pixel value. M represents the number of layers in the pre-trained network. H_i, W_i are the height and width of the i -th layer's feature maps. ϕ is the function in VGG. L_i represents the loss function of the i -th stage, $i = 4$ in SMDR-IS.

Final loss functions (L_{all}) used in training SMDR-IS can be written as:

$$L_{all} = \sum_{i=1}^4 L_i \quad (6)$$

Table 1: Quantitative comparison between state-of-the-art methods and the proposed SMDR-IS on different testing sets.

Dataset	Metric	ULAP	IBLA	GDCP	WaterNet	FUnIE-GAN	UWCNN	UColor	PUIE	SMDR-IS
UIEB Val	PSNR \uparrow	15.913	17.988	13.386	17.349	17.114	17.985	20.962	22.133	23.710
	MSE \downarrow	0.174	0.143	0.228	0.144	0.150	0.134	0.097	0.082	0.075
	SSIM \uparrow	0.745	0.805	0.747	0.813	0.701	0.844	0.863	0.895	0.922
	VSI \uparrow	0.947	0.958	0.943	0.966	0.941	0.966	0.971	0.979	0.983
	FSIM \uparrow	0.915	0.928	0.901	0.908	0.891	0.923	0.931	0.954	0.967
	FSIMc \uparrow	0.878	0.899	0.865	0.899	0.858	0.903	0.920	0.944	0.957
	UIQM \uparrow	2.259	2.490	2.670	2.917	3.092	3.011	3.049	3.036	3.015
	UCIQE \uparrow	0.604	0.606	0.592	0.606	0.564	0.554	0.591	0.588	0.607
	CCF \uparrow	24.145	23.841	23.026	20.042	20.416	20.360	21.827	23.855	26.012
	CEIQ \uparrow	3.209	3.283	3.208	3.101	3.307	3.090	3.209	3.336	3.369
UIEB Test	ALL \uparrow	49.441	51.656	46.109	47.455	47.733	48.502	53.226	56.638	60.466
	UIQM \uparrow	1.511	1.834	2.110	2.399	2.867	2.514	2.481	2.548	2.574
	UCIQE \uparrow	0.569	0.607	0.583	0.591	0.556	0.530	0.565	0.573	0.578
	CCF \uparrow	16.726	20.250	18.573	16.279	16.283	14.996	16.825	19.009	19.740
	CEIQ \uparrow	2.784	3.180	3.121	2.983	2.967	2.836	3.053	3.249	3.188
U45	ALL \uparrow	21.589	25.872	24.387	22.252	22.673	20.876	22.925	25.378	26.081
	UIQM \uparrow	2.282	2.388	2.275	2.957	2.495	3.064	3.148	3.192	3.121
	UCIQE \uparrow	0.588	0.595	0.597	0.601	0.545	0.554	0.586	0.581	0.605
	CCF \uparrow	22.069	21.598	22.736	20.391	12.931	21.418	22.100	23.154	25.489
	CEIQ \uparrow	3.192	3.249	3.191	3.186	2.785	3.213	3.283	3.359	3.397
	ALL \uparrow	28.131	27.830	28.799	27.135	18.757	28.248	29.117	30.287	32.612

Experiments

Datasets

We trained SMDR-IS using the UIEB, comprising 800 images for training and 90 paired images for testing. To evaluate the robustness of SMDR-IS, we also conducted tests in various datasets, including UIEB Val, UIEB Test, and U45.

Implementation Details

Our method was implemented using PyTorch, with computations performed on the NVIDIA Tesla V100 GPU, Intel(R) Xeon(R) Silver 4114 CPU, and 32GB RAM. During the training process, we employed a batch size of 44 and set the learning rate to 0.0002. Images were randomly cropped to a size of 256 \times 256 for training. Techniques such as border padding were utilized to ensure that during testing, SMDR-IS is capable of producing results that match the dimensions of the original images.

Comparison Results

In this section, we employed both objective assessments (UIQM, UCIQE (Jiang et al. 2022a), CCF (Wang et al. 2018), CEIQ (Fang et al. 2014), VSI (Zhang, Shen, and Li 2014), PSNR (Korhonen and You 2012), MSE, SSIM (Wang et al. 2004), FSIM, FSIMc (Zhang et al. 2011)) and subjective evaluations to comprehensively analyze.

We conducted comparisons with SOTA methods to validate the superiority of SMDR-IS, including traditional methods (ULAP (Song et al. 2018), IBLA (Peng and Cosman 2017), GDCP (Peng, Cao, and Cosman 2018)) and deep learning methods (WaterNet (Li et al. 2019), FUnIE-GAN (Islam, Xia, and Sattar 2020), UWCNN (Li, Anwar, and

Porikli 2020), UColor (Li et al. 2021), and PUIE (Fu et al. 2022b)). The subjective results are shown in Figure 4, while the objective results are presented in Table 1.

To avoid the impact of color on metrics (e.g., ULAP in Figure 4), we excluded the color component in CCF. As observed in Figure 4, SMDR-IS excels in both visual quality and metrics. ULAP, IBLA, and GDCP achieve reasonable image restoration but suffer from limited generalization due to the reliance on prior. WaterNet and UColor exhibit better robustness, yet are still influenced by extra input. FUnIE-GAN and UWCNN show real-time but face limitations in expressive power due to small parameters. Although PUIE demonstrates a degree of generalization, it still exhibits overexposure effects (row 8 of Figure 4).

To avoid errors caused by individual metrics, we introduced all metrics in Table 1, where ALL is the sum of \uparrow minus \downarrow values. ALL provides a comprehensive evaluation by considering multiple criteria. SMDR-IS achieves the best score in ALL. Overall, SMDR-IS demonstrates efficacy in restoring complex scenes through synergistic multiscale detail extraction and intrinsic supervision.

Efficiency Evaluation

Table 2 presents a comparative analysis of efficiency, metric (from the UIEB Val in Table 1), and Aggregative. While SMDR-IS might not achieve the highest efficiency, it still achieves a commendable frame rate of 16.4744FPS, meeting real-time requirements. Moreover, we introduce the Aggregative to provide a holistic performance assessment, which evaluates both efficiency and metrics, specifically Aggregative = Metric-Time. In Table 2, SMDR-IS achieves the highest in the Aggregative, which demonstrates the suitabil-

Table 2: Aggregative evaluation of efficiency and metric.

	ULAP	IBLA	GDCP	WaterNet	FUnIE GAN	UWCNN	UColor	PUIE	SMDR-IS
Time ↓	0.3583	9.1341	0.1625	0.0906	0.0033	0.0497	0.5765	0.0181	0.0607
Metric ↑	49.441	51.656	46.109	47.455	47.733	48.502	53.226	56.638	60.466
Aggregative ↑	49.0827	42.5219	45.9465	47.3644	47.7297	48.4523	52.6495	56.6199	60.4053

ity of SMDR-IS for advanced underwater vision tasks.

Ablation Study

We conducted ablation experiments on the testing set of the UIEB dataset. We degraded the stages and presented the results in Table 4. Ablation study is also performed on the components within BICA, as shown in Table 5, as well as on ASISF within SMDI-IR, as shown in Table 3, and on the loss functions, as indicated in Table 6. Bold denotes the highest achieved score.

Table 3 shows that the intrinsic guidance provided by ASISF effectively eliminates irrelevant features during the image enhancement process.

Table 3: Ablation study for ASISF.

En	En_to_DE	De	PSNR ↑	SSIM ↑	ALL ↑
	✓	✓	23.021	0.915	23.936
✓		✓	23.697	0.919	24.615
✓	✓		23.122	0.914	24.036
✓	✓	✓	23.710	0.922	24.631

Table 4: Ablation study for the stage. S represents stage.

S1	S2	S3	S4	PSNR ↑	SSIM↑	ALL↑
✓				22.790	0.916	23.706
✓	✓			22.872	0.915	23.787
✓	✓	✓		23.248	0.915	24.163
✓	✓	✓	✓	23.710	0.922	24.631

Table 4 and Figure 5 are evident that the number of stages significantly influences the metrics. As stage number increases, the image restoration performance and multi-scale feature extraction capability of SMDI-IR gradually enhance. When stage=4, the metrics achieve optimal values. It's worth noting that we selected stage=4 with reference to common practices, where three-fold downsampling is frequently employed as indicated in (Li et al. 2021).

Table 5: Ablation study for BICA.

CA	PA	ReGIA	HCAFE	PSNR ↑	SSIM ↑	ALL ↑
	✓	✓	✓	21.219	0.901	22.120
✓		✓	✓	23.352	0.917	24.269
✓	✓		✓	22.673	0.907	23.580
✓	✓	✓		23.276	0.911	24.186
✓	✓	✓	✓	23.710	0.922	24.631

The effectiveness of BICA architecture is showcased in Table 5, revealing the benefits of each module's restorative

impact through ablative experiments within BICA. However, the impact of the proposed ReGIA on SMDI-IR stands out, thus validating the superiority of ReGIA. Moreover, to validate the effectiveness of the employed loss functions in the paper, we conducted ablation experiments by individually removing L_1 , L_{pre} , and L_{mse} in Table 6, thereby confirming the efficacy of loss function.

Table 6: Ablation study for loss function.

L_1	L_{pre}	L_{mse}	PSNR↑	SSIM↑	ALL↑
	✓	✓	23.257	0.915	24.172
✓		✓	22.905	0.912	23.817
✓	✓		23.151	0.919	24.069
✓	✓	✓	23.710	0.922	24.631

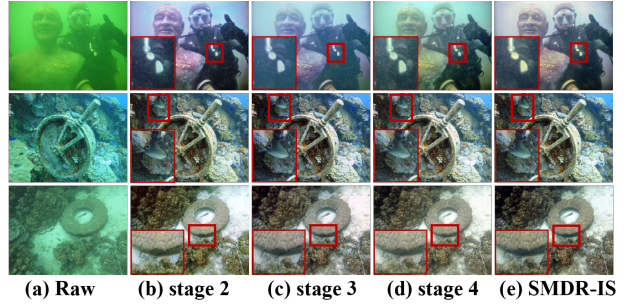


Figure 5: The subjective result for the ablated stages. From left to right: (a) raw images, (b)-(e) correspond to lines 1-4 in Table 4, and (f) ground-truth.

Conclusion

SMDR-IS provides multi-scale scene information based on the multi-resolution framework, synergistic multiscale detail extraction, and intrinsic supervision, which utilize the scale-related features inherent in image scenes. To integrate and optimally leverage the information from multi-scales, we incorporate inputs from the low-resolution within the original resolution, which enhances the transfer of scene information. To mitigate irrelevant scene interference, ASISF is designed to govern the feature propagation process. The multi-degradation loss function is employed to constrain the network's training process. Each stage's optimization and constraints enhance the network's ability to utilize different scale information. In summary, SMDR-IS effectively harnesses multi-scale scenes to enhance various scene information in underwater images.

References

Fang, Y.; Ma, K.; Wang, Z.; Lin, W.; Fang, Z.; and Zhai, G. 2014. No-reference quality assessment of contrast-distorted images based on natural scene statistics. *IEEE Signal Processing Letters*, 22(7): 838–842.

Fu, Z.; Lin, H.; Yang, Y.; Chai, S.; Sun, L.; Huang, Y.; and Ding, X. 2022a. Unsupervised Underwater Image Restoration: From a Homology Perspective. In *AAAI*, volume 36, 643–651.

Fu, Z.; Wang, W.; Huang, Y.; Ding, X.; and Ma, K.-K. 2022b. Uncertainty Inspired Underwater Image Enhancement. In *Computer Vision–ECCV 2022: 17th European Conference, Tel Aviv, Israel, October 23–27, 2022, Proceedings, Part XVIII*, 465–482. Springer.

Guo, C.; Wu, R.; Jin, X.; Han, L.; Zhang, W.; Chai, Z.; and Li, C. 2023. Underwater Ranker: Learn Which is Better and How to Be Better. In *AAAI*, volume 37, 702–709.

Hou, G.; Li, N.; Zhuang, P.; Li, K.; Sun, H.; and Li, C. 2023. Non-uniform Illumination Underwater Image Restoration via Illumination Channel Sparsity Prior. *IEEE Transactions on Circuits and Systems for Video Technology*.

Islam, M. J.; Xia, Y.; and Sattar, J. 2020. Fast Underwater Image Enhancement for Improved Visual Perception. *IEEE Robotics and Automation Letters*, 5(2): 3227–3234.

Jiang, K.; Wang, Z.; Yi, P.; Chen, C.; Huang, B.; Luo, Y.; Ma, J.; and Jiang, J. 2020. Multi-scale Progressive Fusion Network for Single Image Deraining. In *CVPR*, 8346–8355.

Jiang, Q.; Gu, Y.; Li, C.; Cong, R.; and Shao, F. 2022a. Underwater Image Enhancement Quality Evaluation: Benchmark Dataset and Objective Metric. *IEEE Transactions on Circuits and Systems for Video Technology*, 32(9): 5959–5974.

Jiang, Z.; Li, Z.; Yang, S.; Fan, X.; and Liu, R. 2022b. Target Oriented Perceptual Adversarial Fusion Network for Underwater Image Enhancement. *IEEE Transactions on Circuits and Systems for Video Technology*, 32(10): 6584–6598.

Kang, Y.; Jiang, Q.; Li, C.; Ren, W.; Liu, H.; and Wang, P. 2022. A Perception-aware Decomposition and Fusion Framework for Underwater Image Enhancement. *IEEE Transactions on Circuits and Systems for Video Technology*, 33(3): 988–1002.

Korhonen, J.; and You, J. 2012. Peak Signal-to-noise Ratio Revisited: Is Simple Beautiful? In *QoMEx*, 37–38. IEEE.

Li, C.; Anwar, S.; Hou, J.; Cong, R.; Guo, C.; and Ren, W. 2021. Underwater Image Enhancement via Medium Transmission-guided Multi-color Space Embedding. *IEEE Transactions on Image Processing*, 30: 4985–5000.

Li, C.; Anwar, S.; and Porikli, F. 2020. Underwater Scene Prior Inspired Deep Underwater Image and Video Enhancement. *Pattern Recognition*, 98: 107038.

Li, C.; Guo, C.; Ren, W.; Cong, R.; Hou, J.; Kwong, S.; and Tao, D. 2019. An Underwater Image Enhancement Benchmark Dataset and Beyond. *IEEE Transactions on Image Processing*, 29: 4376–4389.

Liu, J.; Shang, J.; Liu, R.; and Fan, X. 2022a. Attention-guided Global-local Adversarial Learning for Detail-preserving Multi-exposure Image Fusion. *IEEE Transactions on Circuits and Systems for Video Technology*, 32(8): 5026–5040.

Liu, J.; Wu, G.; Luan, J.; Jiang, Z.; Liu, R.; and Fan, X. 2023. HoLoCo: Holistic and Local Contrastive Learning Network for Multi-exposure Image Fusion. *Information Fusion*, 95: 237–249.

Liu, R.; Jiang, Z.; Yang, S.; and Fan, X. 2022b. Twin Adversarial Contrastive Learning for Underwater Image Enhancement and Beyond. *IEEE Transactions on Image Processing*, 31: 4922–4936.

Peng, Y.-T.; Cao, K.; and Cosman, P. C. 2018. Generalization of the Dark Channel Prior for Single Image Restoration. *IEEE Transactions on Image Processing*, 27(6): 2856–2868.

Peng, Y.-T.; and Cosman, P. C. 2017. Underwater Image Restoration Based on Image Blurriness and Light Absorption. *IEEE transactions on image processing*, 26(4): 1579–1594.

Song, W.; Wang, Y.; Huang, D.; and Tjondronegoro, D. 2018. A Rapid Scene Depth Estimation Model based on Underwater Light Attenuation Prior for Underwater Image Restoration. In *Pacific Rim Conference on Multimedia*, 678–688. Springer.

Wang, Y.; Guo, J.; Gao, H.; and Yue, H. 2021. UIEC²-Net: CNN-based Underwater Image Enhancement using Two Color Space. *Signal Processing: Image Communication*, 96: 116250.

Wang, Y.; Li, N.; Li, Z.; Gu, Z.; Zheng, H.; Zheng, B.; and Sun, M. 2018. An Imaging-inspired No-reference Underwater Color Image Quality Assessment Metric. *Computers & Electrical Engineering*, 70: 904–913.

Wang, Z.; Bovik, A. C.; Sheikh, H. R.; and Simoncelli, E. P. 2004. Image Quality Assessment: From Error Visibility to Structural Similarity. *IEEE Transactions on Image Processing*, 13(4): 600–612.

Zamir, S. W.; Arora, A.; Khan, S.; Hayat, M.; Khan, F. S.; Yang, M.-H.; and Shao, L. 2021. Multi-stage Progressive Image Restoration. In *CVPR*, 14821–14831.

Zhang, D.; Zhou, J.; Zhang, W.; Lin, Z.; Yao, J.; Polat, K.; Alenezi, F.; and Alhudhaif, A. 2023. ReX-Net: A Reflectance-guided Underwater Image Enhancement Network for Extreme Scenarios. *Expert Systems with Applications*, 120842.

Zhang, L.; Shen, Y.; and Li, H. 2014. VSI: A Visual Saliency-induced Index for Perceptual Image Quality Assessment. *IEEE Transactions on Image processing*, 23(10): 4270–4281.

Zhang, L.; Zhang, L.; Mou, X.; and Zhang, D. 2011. FSIM: A Feature Similarity Index for Image Quality Assessment. *IEEE Transactions on Image Processing*, 20(8): 2378–2386.

Zhou, J.; Li, B.; Zhang, D.; Yuan, J.; Zhang, W.; Cai, Z.; and Shi, J. 2023a. UGIF-Net: An Efficient Fully Guided Information Flow Network for Underwater Image Enhancement. *IEEE Transactions on Geoscience and Remote Sensing*.

Zhou, J.; Pang, L.; Zhang, D.; and Zhang, W. 2023b. Underwater Image Enhancement Method via Multi-interval Subhistogram Perspective Equalization. *IEEE Journal of Oceanic Engineering*.

Zhou, J.; Sun, J.; Zhang, W.; and Lin, Z. 2023c. Multi-view Underwater Image Enhancement Method via Embedded Fusion Mechanism. *Engineering Applications of Artificial Intelligence*, 121: 105946.

Zhou, J.; Zhang, D.; Ren, W.; and Zhang, W. 2022. Auto Color Correction of Underwater Images Utilizing Depth Information. *IEEE Geoscience and Remote Sensing Letters*, 19: 1–5.

Zhou, J.; Zhang, D.; and Zhang, W. 2023. Cross-view Enhancement Network for Underwater Images. *Engineering Applications of Artificial Intelligence*, 121: 105952.

Zhuang, P.; Li, C.; and Wu, J. 2021. Bayesian Retinex Underwater Image Enhancement. *Engineering Applications of Artificial Intelligence*, 101: 104171.

Zhuang, P.; Wu, J.; Porikli, F.; and Li, C. 2022. Underwater Image Enhancement with Hyper-laplacian Reflectance Priors. *IEEE Transactions on Image Processing*, 31: 5442–5455.